Scilight

Applied Nonlinear Dynamics and Vibrations
https://www.sciltp.com/journals/andv

Check for updates

Review

Review of Multiaxial Vibration Fatigue Spectral Methods—With Open-Source Support

Jaša Šonc and Janko Slavič *

Faculty of Mechanical Engineering, University of Ljubljana, Aškerčeva 6, 1000 Ljubljana, Slovenia
* Correspondence: janko.slavic@fs.uni-lj.si

How To Cite: Šonc, J.; Slavič, J. Review of Multiaxial Vibration Fatigue Spectral Methods—With Open-Source Support. *Applied Nonlinear Dynamics and Vibrations* **2026**, *1*(1), 3. https://doi.org/10.53941/andv.2026.100003

Received: 20 April 2026
Revised: 27 May 2026
Accepted: 3 June 2026
Published: 9 June 2026

Abstract: In vibration fatigue, dynamic excitation such as base acceleration or force can produce a multiaxial stress response. In the frequency domain, this stress response is characterised by a cross-power-spectral-density (cross-PSD) matrix that contains the spectral content of each stress component and the phase relations between them. For fatigue-life estimation under stationary excitation, the multiaxial stress cross-PSD is reduced to an equivalent uniaxial stress PSD compatible with established spectral damage models. Several criteria have been proposed for this reduction, each differing in the assumptions made about phase relations, the required material parameters, and computational cost. This paper provides an implementation-oriented review of ten such criteria: three critical-plane variants (maximum normal, maximum shear, and combined normal-and-shear stress), the equivalent von Mises stress and its adaptation for out-of-phase stress components, the Carpinteri–Spagnoli frequency-domain reformulation, the frequency-based multiaxial rainflow, a thermoelasticity-based criterion, the Niesłony hydrostatic–deviatoric combination, and the equivalent Lemaitre stress with multiaxial S–N interpolation. As a result of this research, all ten methods are also implemented in `FLife` (version 2.2.0), an open-source Python package that extends the uniaxial spectral framework to multiaxial inputs. Previously these implementations were distributed across separate source papers; here they share a single input format and a single workflow, so that any subset can be compared on the same dataset without reimplementation. A comparative overview highlights trade-offs between simplicity, sensitivity to non-proportional loading, material-parameter requirements, and computational cost, supporting method selection in multiaxial vibration-fatigue practice. The criteria are also applied to a common dataset, where the equivalent stress varies by up to about a factor of 1.7 across the ten criteria.

Keywords: multiaxial vibration fatigue; spectral methods; equivalent stress; power spectral density; open source; reproducibility; `FLife`

1. Introduction

High-cycle fatigue under random vibration loading remains a fundamental durability concern for many engineering structures and components [1,2]. Traditional fatigue-life assessment is often performed in the time domain, where long stress histories are processed by cycle counting and cumulative damage rules [3]. For large numerical models, multiple load cases, or long-duration recordings, this workflow can become computationally demanding. Multiaxial fatigue has a longer history than the spectral methods reviewed here. Garud's 1981 survey already listed dozens of constant-amplitude criteria [4]. Frequency-domain (spectral) methods address the cost of time-domain processing by working directly with response power spectral densities (PSDs) and well-established random-process theory [5,6], enabling efficient life estimation [2]; comparative assessments of such methods can be found in [7]. In multiaxial vibration settings, spectral methods are especially attractive because the random-response finite-element method (FEM) readily provides stress PSDs at many points, which can be mapped to fatigue-relevant scalar measures [8,9]; for a broader overview see [10]. This is particularly relevant for modern qualification and durability workflows where multi-axis excitations and correlated

Copyright: © 2026 by the authors. This is an open access article under the terms and conditions of the Creative Commons Attribution (CC BY) license (https://creativecommons.org/licenses/by/4.0/).
Publisher's Note: Scilight stays neutral with regard to jurisdictional claims in published maps and institutional affiliations.

inputs are routinely prescribed or measured, motivating multiaxial spectral formulations [11] and multiaxial extensions of damage-spectrum concepts [12,13].

These spectral methods began as uniaxial damage estimators. They predict fatigue damage directly from the stress PSD, with no reconstructed time history. Rychlik [14] gave a precise definition of the rainflow counting that these estimators approximate. Wirsching and Light [15] gave an early wide-band estimator, relating damage to the spectral moments of the PSD through an empirical correction. Dirlik [16] fitted an empirical closed-form expression for the rainflow-amplitude distribution that holds for a range of spectral shapes. Bishop and Sherratt [17] took a different route and derived the distribution of rainflow ranges from the PSD analytically. Tovo and Benasciutti [18] combined the narrow-band and range-counting limits into one wide-band estimator. Braccesi and Cianetti [19] extended the approach to bimodal stress processes. Book-length treatments of vibration fatigue and the fatigue-damage spectrum are given by Lalanne [1]. These uniaxial models are reviewed by Zanardi et al. [20]; Slavič et al. cover them in a monograph [21].

When the stress state is multiaxial, the key additional step is to reduce the tensor-valued stress process to a scalar equivalent process compatible with uniaxial spectral damage models. A seminal milestone is the equivalent von Mises stress (EVMS) formulation by Preumont and Piéfort [22], which combines stress (cross-)PSDs through a quadratic von Mises operator. Subsequent developments clarified accuracy and limits of EVMS-type reductions and motivated extensions that account for correlation and phase relations between tensor components [23,24]; see also [10]. More general frequency-domain multiaxial formulations (e.g., based on critical-plane ideas and invariant criteria) were shown to achieve accuracy comparable to time-domain multiaxial analyses while preserving the computational advantages of spectral evaluation [8,25], including stress-invariant [26] and comparative [7] approaches. Niesłony [27] later compared several of these spectral multiaxial criteria. Łagoda et al. [28] developed an energy-based critical-plane approach for multiaxial random loading. These approaches differ primarily in how the stress cross-PSD matrix (including coherence and phase) is used to build an equivalent scalar process that remains compatible with uniaxial random-fatigue models [24,26]; a detailed discussion is given in [10].

Recent comparative studies and reviews emphasise that multiaxial spectral criteria can yield different life predictions under non-proportional loading and correlated stress components, so assumptions and applicability must be stated clearly [9,25], as highlighted in dedicated reviews [3,29] and recent comparative studies [10]. In parallel, vibration-test tailoring and spectrum-based durability metrics continue to evolve for accelerated qualification and environment comparison. For example, sine-on-random profile design has been studied through fatigue-damage-spectrum (FDS) equivalence [30], while recent studies extend these ideas to explicitly multiaxial formulations [11, 13], including multi-axis versus single-axis comparisons [12]. Spectral evaluation relies on linear-system response and stationary Gaussian assumptions [5]; deviations from these conditions may require additional validation [2,3]. Wolfsteiner and Breuer [31] studied non-Gaussian random-vibration fatigue from power spectral densities. Recent work has begun addressing these limitations: higher-order and modal-domain spectral characterisations have been proposed for non-Gaussian loads [32,33], efficient methods for computing non-Gaussian response statistics have been developed [34,35], and mean-stress corrections have been integrated into non-Gaussian spectral damage models [36, 37]. Beyond non-Gaussian extensions, spectral fatigue methods are being applied to increasingly complex structural contexts, including notched components [38], welded joints [39], and superalloy components and marine structures under bimodal random loading [40,41]. At the same time, reproducibility and transparent implementations are increasingly important: open-source packages enable consistent comparisons across criteria and facilitate adoption in both research and industrial workflows [42,43].

This article focuses on multiaxial spectral criteria relevant to vibration fatigue and provides a concise, implementation-oriented description of principal approaches (EVMS and phase-aware variants, critical-plane methods in the frequency domain, Carpinteri–Spagnoli, frequency-based multiaxial rainflow, thermoelasticity-based criteria, hydrostatic–deviatoric combinations, Lemaitre-based equivalents). To support reproducible vibration-fatigue analysis, the open-source Python package `FLife` was established in 2020 and introduced in the review and open-source comparison framework by Zorman et al. [42]. This paper is a continuation of that effort and focuses specifically on the multiaxial upgrade of `FLife`: the new multiaxial workflow is documented and it is shown how multiaxial stress PSDs are converted to an equivalent uniaxial PSD and then evaluated with uniaxial spectral damage models in a single consistent pipeline [43].

There are already review-style contributions on multiaxial spectral fatigue: Muñiz-Calvente et al. compared time- and frequency-domain methods [3], Benasciutti et al. surveyed developments through the mid-2010s [10], and Carpinteri et al. reviewed criteria for random variable-amplitude loading [29]. None of these reviews provides an implementation. Applying several criteria to the same dataset still requires re-implementing each from its source paper. The main contribution of this paper is therefore the implementation: ten criteria written in consistent notation,

including recent additions [44–48], released as a single open-source workflow [43]. Building on it, the paper also compares the ten criteria on a common dataset, to show how much the criterion choice changes the result and to make the capabilities of the package reproducible, while a full experimental accuracy benchmark across materials and loading types is left to future work.

2. Critical Plane Criteria

2.1. Maximum-Stress Criteria on a Critical Plane (Spectral Form)

A widely used class of multiaxial critical-plane approaches assumes that fatigue is governed by stress components acting on a material plane whose orientation must be identified. Findley proposed the first normal-and-shear critical-plane criterion in 1959 [49], and Brown and Miller introduced the strain-based critical-plane framework in 1973 [50]. In the spectral formulation of Niesłony and Macha [25], the equivalent stress PSD on a candidate plane is obtained as the scalar output of a six-input linear system driven by the stress cross-PSD matrix $\mathbf{S}_{ss}(\omega)$ [25]:

$$S_{\mathrm{eq}}(\omega) = \mathbf{a}\,\mathbf{S}_{ss}(\omega)\,\mathbf{a}^{T}. \tag{1}$$

Different choices of the coefficient vector $\mathbf{a}$ yield the three variants commonly reported in the spectral critical-plane literature: maximum normal stress, maximum shear stress, and a combined maximum normal-and-shear stress criterion [25]. The coefficients are functions of the plane orientation and are typically expressed through directional cosines of the principal stress axes (e.g., l_i, m_i, n_i). The combined form introduces a material coefficient [51]:

$$K = 2\frac{\tau_{af}}{\sigma_{af}} - 1, \tag{2}$$

defined from the fully reversed torsion and bending fatigue limits. For each plane orientation, Equation (1) provides a scalar equivalent PSD, which can be evaluated with a uniaxial spectral damage model (e.g., via spectral moments and a chosen bandwidth correction).

Critical Plane Selection in a Spectral Workflow

(i) Damage Accumulation Scan (Plane-by-Plane).

A discrete set of plane orientations is sampled; for each plane, the equivalent stress PSD is obtained from the stress cross-PSD matrix via

$$S_{\mathrm{eq}}(\omega) = \mathbf{a}\,\mathbf{S}_{ss}(\omega)\,\mathbf{a}^{T}, \tag{3}$$

and a uniaxial spectral damage model is applied to compute the fatigue life. The critical plane is then defined as the orientation that maximises the predicted damage. This procedure is consistent with the original critical-plane philosophy (damage governed by the most damaging plane), but can be computationally demanding when many orientations and many spatial points must be evaluated [25].

(ii) Maximum-Variance Plane (Computationally Efficient).

A numerically cheaper alternative to the full-scan approach replaces the frequency-by-frequency scan by searching for the plane that maximises the variance of the equivalent stress associated with the selected critical-plane mapping [25]. Introducing the 6×6 covariance matrix $\mathbf{C}$ of the stress components (obtained by integrating $\mathbf{S}_{ss}(\omega)$), the variance becomes [25]:

$$\sigma_{\mathrm{eq}}^{2} = \mathrm{Var}[s_{\mathrm{eq}}] = \mathbf{a}\,\mathbf{C}\,\mathbf{a}^{T}, \tag{4}$$

and the critical plane is obtained by maximising σ_{eq}^{2} over all orientations. This removes the explicit frequency dependence from the critical-plane search (only scalar covariances are required), substantially accelerating large-scale random-response FEM applications [25]. A commonly used special case is to identify the critical plane from the maximum shear-stress variance, consistent with Matake's concept [52]. As noted by Niesłony and Macha [25], the variance-based approach is most reliable when the stress components exhibit consistent probabilistic characteristics (e.g., Gaussian assumptions typical for linear random vibration).

3. EVMS (Equivalent von Mises Stress)

The frequency-domain formulation of the von Mises criterion, commonly known as the EVMS criterion, reduces a multiaxial stress response to an equivalent uniaxial power spectral density (PSD), without introducing a critical-plane search. The frequency-domain formulation was proposed by Preumont and Piéfort [22]. The equivalent PSD is obtained by a quadratic combination of the tensor components directly in the spectral domain,

yielding a single scalar spectrum that preserves the mean-square equivalent from the time domain to the frequency domain [9,22]:

$$\widetilde{S}_c(\omega) = \mathrm{Trace}[\mathbf{Q}\,\mathbf{S}_{ss}(\omega)]\,. \tag{5}$$

where $\mathbf{Q}$ is the coefficient matrix:

$$\mathbf{Q} = \begin{bmatrix} 1 & -1/2 & -1/2 & 0 & 0 & 0 \\ -1/2 & 1 & -1/2 & 0 & 0 & 0 \\ -1/2 & -1/2 & 1 & 0 & 0 & 0 \\ 0 & 0 & 0 & 3 & 0 & 0 \\ 0 & 0 & 0 & 0 & 3 & 0 \\ 0 & 0 & 0 & 0 & 0 & 3 \end{bmatrix} \tag{6}$$

Equation (5) is widely used due to its simplicity and straightforward integration with random-response FEM workflows [9]. A known limitation is that the classical EVMS formulation can overestimate the equivalent von Mises level when stress components are out of phase, which motivated subsequent corrections by Bonte et al. [24] and analytical investigations by Benasciutti [23]; see also [27].

4. Carpinteri-Spagnoli Criterion

The Carpinteri–Spagnoli (C–S) approach is a critical-plane multiaxial criterion originally proposed for high-cycle fatigue [53], where the fatigue-relevant plane is not obtained by maximizing an instantaneous stress component, but is correlated with averaged principal stress directions [54]. For random multiaxial loading, Carpinteri et al. later reformulated the criterion directly in the frequency domain by determining the critical-plane orientation from the stress-tensor PSD matrix, avoiding explicit time-history processing [53]. After the critical plane is identified, the multiaxial stress state on that plane is reduced to a scalar equivalent PSD by combining the PSD of the normal stress and the PSD of a suitably projected shear stress acting on the plane (projected along the direction of maximum variance) [53]. In the notation commonly adopted in spectral implementations, with x, y lying in the critical plane and z normal to it, and with S_{yz} denoting the PSD of the projected shear stress (projected along the direction of maximum variance on the plane), the equivalent spectrum is defined as [9]:

$$S_{\mathrm{eq}}(\omega) = S_{zz}(\omega) + \left(\frac{\sigma_{\mathrm{fr}}}{\tau_{\mathrm{fr}}}\right) S_{yz}(\omega), \tag{7}$$

where σ_{fr} and τ_{fr} are the fully reversed bending- and torsion-fatigue limits, respectively. The resulting scalar PSD is then processed by a uniaxial spectral damage model (e.g., Tovo–Benasciutti) to estimate fatigue life [53].

5. Frequency-Based Multiaxial Rainflow Criterion

Rainflow cycle counting originates with Matsuishi and Endo [55,56]. The multiaxial extensions below adapt this scalar-process counting idea to non-proportional stress histories. Pitoiset and Preumont [8] showed that the multiaxial rainflow concept can be implemented efficiently in the frequency domain in a form closely analogous to EVMS. The method is based on constructing a family of scalar stress processes as linear combinations of the local stress tensor components,

$$s_m(t) = \mathbf{c}^T \mathbf{s}(t), \qquad \|\mathbf{c}\| = 1, \tag{8}$$

where $\mathbf{c}$ is a unit direction vector in the stress-component space and $\mathbf{s}(t)$ is the stress vector, and evaluating fatigue damage for each combination; the most damaging direction $\mathbf{c}$ is then taken as the governing direction [57,58], as formalised by Pitoiset and Preumont [8]. For a stationary process, the scalar PSD associated with a given $\mathbf{c}$ can be obtained directly from the stress cross-PSD matrix (here denoted $\mathbf{F}_{ss}(\omega)$ following Pitoiset and Preumont's notation, equivalent to $\mathbf{S}_{ss}(\omega)$ used in the preceding sections):

$$F_m(\omega) = \mathrm{Trace}(\mathbf{Q}^*\,\mathbf{F}_{ss}(\omega))\,, \qquad \mathbf{Q}^* = \mathbf{c}\,\mathbf{c}^T, \tag{9}$$

so that the multiaxial rainflow search becomes a scan over unit direction vectors $\mathbf{c}$ in the spectral domain [8]. In practical spectral fatigue workflows, $F_m(\omega)$ is passed to a chosen uniaxial spectral damage model (e.g. moment-based methods) and the maximum predicted damage over the set of $\mathbf{c}$ is retained [8]. In its current spectral formulation, the method has been developed for biaxial (plane-stress) states. Compared to time-domain implementations that require explicit multichannel cycle counting, the frequency-domain formulation offers large computational savings

while preserving the core "most damaging combination" idea of the original multiaxial rainflow approach [8].

6. Thermoelasticity-Based Criterion

While the preceding criteria rely on numerical stress fields from finite-element models, experimental full-field stress data can also serve as input for spectral fatigue analysis. Infrared thermography offers a non-contact way to obtain such data in real time, motivating a fatigue criterion built directly on the measured thermoelastic signal. Thermoelastic stress analysis (TSA) uses the reversible thermoelastic effect: under (approximately) adiabatic elastic conditions, the measured temperature variation is proportional to the first invariant of the stress tensor [59,60]. The scalar thermoelastic response can be written as

$$\frac{\Delta T}{K_m} = \sigma_{xx} + \sigma_{yy} + \sigma_{zz}, \tag{10}$$

so an infrared (IR) camera provides a full-field measurement of the sum of normal stresses on the observed surface, including their sign (via the complex frequency-domain representation) [46].

For multiaxial random vibration, Šonc et al. [46] propose treating the thermoelastic scalar as an equivalent uniaxial stress process in the frequency domain, analogous to equivalent-stress spectral methods. Let $\mathbf{S}_{ss}(\omega)$ be the 6×6 cross-PSD matrix of $\boldsymbol{\sigma}(t) = [\sigma_x, \sigma_y, \sigma_z, \tau_{xy}, \tau_{xz}, \tau_{yz}]^T$. The equivalent thermoelastic stress PSD is defined as

$$S_{\text{thermo}}(\omega) = \text{Trace}[\mathbf{Q}_{\text{thermo}} \cdot \mathbf{S}_{ss}(\omega)]\,, \tag{11}$$

with the coefficient matrix

$$\mathbf{Q}_{\text{thermo}} = \begin{bmatrix} 1 & 1 & 1 & 0 & 0 & 0 \\ 1 & 1 & 1 & 0 & 0 & 0 \\ 1 & 1 & 1 & 0 & 0 & 0 \\ 0 & 0 & 0 & 0 & 0 & 0 \\ 0 & 0 & 0 & 0 & 0 & 0 \\ 0 & 0 & 0 & 0 & 0 & 0 \end{bmatrix}. \tag{12}$$

The resulting scalar PSD can be directly passed to standard uniaxial spectral damage models. Since only normal stresses enter Equation (11), the criterion is insensitive to pure shear on the surface (e.g., $\sigma_1 = -\sigma_2$) and may underestimate damage when shear contributions are significant; conversely, it is effective when normal stresses dominate (e.g., bending) [46].

7. EVMS Adaptation for Out-of-Phase Components

In random vibration driven by multiple correlated excitations, stress cross-PSDs are generally complex numbers and phase differences between tensor components may occur [24]. Bonte et al. revisit the EVMS procedure of Preumont and Piéfort [22] and show that the classical von Mises PSD combination (based on the real part of cross terms) is exact for in-phase components but can overestimate the equivalent von Mises level for out-of-phase in-plane (plane-stress) stresses [24]. They derive an alternative frequency-bin expression that explicitly incorporates phase angles obtained from the stress cross-PSDs, yielding (for each discrete frequency band f_m) an equivalent von Mises PSD consistent with the maximum of the corresponding time-dependent von Mises stress [24]:

$$\begin{aligned} G_{\sigma_{\text{VM}}}(f_m) = {} & \frac{1}{2}\left(\hat{\sigma}_{xx}^2 + \hat{\sigma}_{yy}^2 - \hat{\sigma}_{xx}\hat{\sigma}_{yy}\cos(\phi_{xx} - \phi_{yy}) + 3\hat{\tau}_{xy}^2\right) \\ & + \frac{1}{2}\left|\hat{\sigma}_{xx}^2 + \hat{\sigma}_{yy}^2\, e^{2j(\phi_{yy}-\phi_{xx})} - \hat{\sigma}_{xx}\hat{\sigma}_{yy}\, e^{j(\phi_{yy}-\phi_{xx})} + 3\hat{\tau}_{xy}^2\, e^{2j(\phi_{xy}-\phi_{xx})}\right|, \end{aligned} \tag{13}$$

with amplitudes obtained from the auto-PSDs and phase differences from the cross-PSD arguments:

$$\hat{\sigma}_{xx}^2 = G_{\sigma_{xx}\sigma_{xx}}(f_m), \qquad \hat{\sigma}_{yy}^2 = G_{\sigma_{yy}\sigma_{yy}}(f_m), \qquad \hat{\tau}_{xy}^2 = G_{\tau_{xy}\tau_{xy}}(f_m), \tag{14}$$

$$\hat{\sigma}_{xx}\hat{\sigma}_{yy} = \sqrt{G_{\sigma_{xx}\sigma_{xx}}(f_m)\; G_{\sigma_{yy}\sigma_{yy}}(f_m)}, \qquad \phi_{yy} - \phi_{xx} = \angle\, G_{\sigma_{xx}\sigma_{yy}}(f_m), \qquad \phi_{xy} - \phi_{xx} = \angle\, G_{\sigma_{xx}\tau_{xy}}(f_m). \tag{15}$$

8. Niesłony Criterion, Combining EVMS and Hydrostatic Stresses

Niesłony et al. [44] propose a frequency-domain multiaxial criterion that combines a deviatoric measure (the equivalent von Mises stress, termed EMS by the original authors) with the hydrostatic stress, while explicitly accounting for their statistical dependence. The equivalent uniaxial fatigue process is defined as a weighted sum of

two stochastic processes,

$$\sigma_{\mathrm{eq}}(t) = A\,p(t) + B\,\sigma_{\mathrm{EMS}}(t), \tag{16}$$

where $p(t)$ is the hydrostatic stress, $\sigma_{\mathrm{EMS}}(t)$ is the equivalent von Mises stress, and A, B are weights derived from fatigue-limit conditions [44]. Following Niesłony et al.'s notation (where $\mathbf{G}_\sigma(f)$ denotes the stress cross-PSD matrix, equivalent to $\mathbf{S}_{ss}(\omega)$ with $\omega = 2\pi f$), yields an equivalent PSD according to stochastic summation [5,44]:

$$G_{\mathrm{eq}}(f) = A^2 G_p(f) + B^2 G_{\mathrm{EMS}}(f) + 2AB\,\Re[G_{p,\mathrm{EMS}}(f)]\,. \tag{17}$$

Here, $p(t) = \frac{1}{3}(\sigma_{xx} + \sigma_{yy} + \sigma_{zz})$ and both $G_p(f)$ and $G_{\mathrm{EMS}}(f)$ are obtained directly from the 6×6 stress PSD matrix $\mathbf{G}_\sigma(f)$ via trace operators,

$$G_p(f) = \mathrm{Trace}\{\mathbf{Q}_p\,\mathbf{G}_\sigma(f)\}\,, \qquad \mathbf{Q}_p = \frac{1}{9}\begin{bmatrix} 1 & 1 & 1 & 0 & 0 & 0 \\ 1 & 1 & 1 & 0 & 0 & 0 \\ 1 & 1 & 1 & 0 & 0 & 0 \\ 0 & 0 & 0 & 0 & 0 & 0 \\ 0 & 0 & 0 & 0 & 0 & 0 \\ 0 & 0 & 0 & 0 & 0 & 0 \end{bmatrix}, \tag{18}$$

$$G_{\mathrm{EMS}}(f) = \mathrm{Trace}\{\mathbf{Q}_{\mathrm{EMS}}\,\mathbf{G}_\sigma(f)\}\,, \qquad \mathbf{Q}_{\mathrm{EMS}} = \begin{bmatrix} 1 & -\frac{1}{2} & -\frac{1}{2} & 0 & 0 & 0 \\ -\frac{1}{2} & 1 & -\frac{1}{2} & 0 & 0 & 0 \\ -\frac{1}{2} & -\frac{1}{2} & 1 & 0 & 0 & 0 \\ 0 & 0 & 0 & 3 & 0 & 0 \\ 0 & 0 & 0 & 0 & 3 & 0 \\ 0 & 0 & 0 & 0 & 0 & 3 \end{bmatrix}. \tag{19}$$

Since $G_{p,\mathrm{EMS}}(f)$ cannot be formed directly as a trace of $\mathbf{G}_\sigma(f)$, the real part is reconstructed using a frequency-dependent correlation coefficient,

$$\Re[G_{p,\mathrm{EMS}}(f)] = r_{p,\mathrm{EMS}}(f)\sqrt{G_p(f)\,G_{\mathrm{EMS}}(f)}, \tag{20}$$

where $r_{p,\mathrm{EMS}}(f)$ is obtained by recovering phase relations between stress components from the PSD matrix for each frequency line (via a "reference component" with zero phase) and computing the phase difference between complex p and complex EMS [44]. At each frequency line f_m, one stress component is taken as the reference and given zero phase. Each remaining stress component is assigned a magnitude (from its auto-PSD) and a phase (from the cross-PSD argument with the reference). Complex $p(f_m)$ and $\sigma_{\mathrm{EMS}}(f_m)$ follow from these stress components, and $r_{p,\mathrm{EMS}}(f_m)$ is the cosine of their phase difference. The full procedure is described by Niesłony et al. [44] and implemented in the `Nieslony` method of `FLife` [43]. The weights (A, B) are then derived from axial-tension and pure-torsion limit states in two variants: (i) an equivalent PSD intended for use with the axial SN curve, and (ii) an equivalent PSD intended for use with the torsional SN curve, thereby incorporating the axial-to-torsional fatigue-strength ratio directly into the frequency-domain criterion [44].

9. Equivalent Lemaitre Stress and Multiaxial S–N Curve (Ge et al.)

Ge et al. [45] extend EVMS-type spectral criteria by adopting the equivalent Lemaitre stress from damage mechanics, which explicitly includes the hydrostatic-stress contribution [61]. For a multiaxial stationary stress process described by the 6×6 stress PSD matrix $\mathbf{G}_\sigma(f)$, the PSD of the equivalent Lemaitre stress is obtained directly by a trace operation

$$G_{\sigma^*_{\mathrm{eq}}}(f) = \mathrm{Trace}\{\mathbf{Q}^*\,\mathbf{G}_\sigma(f)\}\,, \tag{21}$$

with the coefficient matrix (Poisson ratio ν)

$$\mathbf{Q}^* = \begin{bmatrix} 1 & -\nu & -\nu & 0 & 0 & 0 \\ -\nu & 1 & -\nu & 0 & 0 & 0 \\ -\nu & -\nu & 1 & 0 & 0 & 0 \\ 0 & 0 & 0 & 2(1+\nu) & 0 & 0 \\ 0 & 0 & 0 & 0 & 2(1+\nu) & 0 \\ 0 & 0 & 0 & 0 & 0 & 2(1+\nu) \end{bmatrix}, \tag{22}$$

which reduces to the EVMS matrix for $\nu = 0.5$ [45]. As noted by the original authors, cross-correlations between normal and shear stresses are ignored in this formulation, analogous to the classical EVMS limitation [45]. The corresponding hydrostatic-stress PSD is formed analogously,

$$G_p(f) = \mathrm{Trace}\{\mathbf{Q}_p\, \mathbf{G}_\sigma(f)\}\,, \qquad \mathbf{Q}_p = \frac{1}{9}\begin{bmatrix} 1 & 1 & 1 & 0 & 0 & 0 \\ 1 & 1 & 1 & 0 & 0 & 0 \\ 1 & 1 & 1 & 0 & 0 & 0 \\ 0 & 0 & 0 & 0 & 0 & 0 \\ 0 & 0 & 0 & 0 & 0 & 0 \\ 0 & 0 & 0 & 0 & 0 & 0 \end{bmatrix}. \tag{23}$$

To avoid the common limitation of EVMS-based approaches that use only the axial S–N curve, Ge et al. construct a multiaxial S–N curve by blending axial (tension–compression) and torsion S–N parameters through a scalar hydrostatic participation factor computed from spectral moments [45]. Defining:

$$q = \frac{3\tilde{p}}{\tilde{\sigma}^*_{\mathrm{eq}}} = 3\frac{\sqrt{m_{0,p}}}{\sqrt{m_{0,\sigma^*_{\mathrm{eq}}}}}, \tag{24}$$

the multiaxial S–N parameters are obtained as a modified Wöhler-type interpolation [62]:

$$k_{\mathrm{app}} = k_{\mathrm{tor}} + q\,(k_{\mathrm{axi}} - k_{\mathrm{tor}})\,, \tag{25}$$

$$\log C_{\mathrm{app}} = \log\!\left(\left(\sqrt{2(1+\nu)}\right)^{k_{\mathrm{tor}}} C_{\mathrm{tor}}\right) + q\Big[\log(C_{\mathrm{axi}}) - \log\!\left(\left(\sqrt{2(1+\nu)}\right)^{k_{\mathrm{tor}}} C_{\mathrm{tor}}\right)\Big], \tag{26}$$

so the final life estimate follows any chosen uniaxial spectral damage model, but evaluated using $G_{\sigma^*_{\mathrm{eq}}}(f)$ together with the multiaxial S–N curve $(C_{\mathrm{app}}, k_{\mathrm{app}})$ [45].

10. Discussion and Open-Source Implementation

The open-source package `FLife` [42,43] extends the uniaxial spectral framework with a multiaxial module implementing the ten criteria reviewed in this article. The workflow reduces the multiaxial stress cross-PSD matrix $\mathbf{S}_{ss}(\omega)$ to an equivalent scalar PSD, which is then passed to any uniaxial spectral damage model already available in the package (e.g. Dirlik, Tovo–Benasciutti, narrowband; see [21]). Multi-point input is supported, enabling full-field fatigue-life maps over finite-element meshes. The criteria differ in how this mapping is constructed and can be grouped into three families: (i) quadratic trace-based reductions that combine PSD components through a fixed coefficient matrix (EVMS, thermoelastic, Lemaitre), (ii) critical-plane projections that search for the most damaging material-plane orientation (maximum normal/shear/combined, Carpinteri–Spagnoli), and (iii) hybrid or dedicated approaches that incorporate additional physical information such as phase angles or hydrostatic–deviatoric decomposition (Bonte out-of-phase correction, Niesłony criterion, frequency-based multiaxial rainflow) [9, 10]. Table 1 summarises the ten criteria with their input requirements, phase sensitivity, and relative computational cost.

For proportional (in-phase) multiaxial loading, the phase-based corrections add little, because the cross-PSD matrix is close to rank-one; the criteria then differ mainly in how they weight the normal and shear contributions rather than through phase [9, 10]. Differences emerge primarily under non-proportional loading, where phase relations between stress components carry information that simpler reductions discard. Bonte et al. [24] introduced an explicit phase correction for the plane-stress case, and Benasciutti [23] later investigated analytically the accuracy of the classical EVMS for out-of-phase components (see also Equation (5)). The Lemaitre formulation [45], while incorporating hydrostatic effects through the Poisson ratio, shares the EVMS limitation of discarding cross-correlations between normal and shear stress components. The Niesłony criterion [44] addresses non-proportionality differently, by explicitly reconstructing the frequency-dependent correlation between hydrostatic and deviatoric measures, although the criterion has so far been validated on constant-amplitude multiaxial specimens and FEM simulations, not yet under broadband random-vibration loading. Zhang et al. [48] recently proposed a damage correction factor that maps uniaxial spectral estimates to multiaxial conditions using the Lemaitre equivalent stress, offering an alternative route to account for load correlation.

Table 1. Overview of multiaxial spectral criteria implemented in `FLife`.

Criterion	Stress Input	Extra Params	Phase	Cost	`FLife` Method
Max. normal stress	3D / 2D	–	partial	High	`max_normal`
Max. shear stress	3D / 2D	–	partial	High	`max_shear`
Max. normal & shear	3D / 2D	σ_{af}, τ_{af}	partial	High	`max_normal_and_shear`
EVMS	3D / 2D	–	no	Low	`EVMS`
Carpinteri–Spagnoli	3D / 2D	σ_{af}, τ_{af}	partial	Med–High	`cs`
Multiaxial rainflow	2D only	–	partial	High	`multiaxial_rainflow`
Thermoelastic	3D / 2D	–	no	Low	`thermoelastic`
EVMS out-of-phase	2D only	–	yes	Medium	`EVMS_out_of_phase`
Niesłony (hydro.+EMS)	3D / 2D	σ_{af}, τ_{af}	yes	Med–High	`Nieslony`
Lemaitre	3D / 2D	ν, axi.+tor. S–N	no	Low	`Lemaitre`

Phase column: no = uses only auto-PSDs; partial = implicitly accounts for cross-PSD structure (e.g. through covariance or projection); yes = explicitly reconstructs phase angles or correlation from cross-PSDs. Cost is relative: Low ≈ single matrix operation per frequency; High ≈ orientation optimisation at each spatial point.

The criteria also differ in the number of material parameters required beyond a uniaxial S–N curve (see Table 1). Several criteria operate without extra material data, while the critical-plane and Carpinteri–Spagnoli formulations require fully reversed bending and torsion fatigue limits (σ_{af}, τ_{af}), and the Lemaitre criterion [45] requires both axial and torsional S–N curve parameters together with the Poisson ratio ν. In industrial practice, these additional parameters are not always readily available, which may favour the simpler criteria as a first estimate. Computational cost ranges from negligible for trace-based methods (a single matrix multiplication per frequency) to significant for critical-plane methods that must optimise over plane orientations at each spatial point; the variance-based shortcut [25] mitigates this by working with the covariance matrix rather than scanning individual frequencies. The frequency-based multiaxial rainflow is the most expensive, as it requires a damage evaluation for each candidate direction $\mathbf{c}$ [8]. For large finite-element models with many evaluation points, these cost differences become practically relevant. Data-driven approaches that directly learn the mapping from PSD features to fatigue damage have also been explored as an alternative to closed-form criteria [47].

Two criteria currently accept only biaxial (plane-stress) input: the Bonte out-of-phase formulation and the frequency-based multiaxial rainflow. Closed-form three-dimensional generalisations remain an open problem. For critical-plane methods, the plane-orientation search in `FLife` supports both a local gradient-based optimiser and a global differential-evolution strategy [43].

10.1. Numerical Comparison

To compare the criteria quantitatively, all ten were applied to two stress cross-PSD datasets taken from the finite-element vibration-fatigue study of Mršnik et al. [9] on an AlSi7Cu3 component: a normal-stress-dominated state, and a combined bending and torsion state built from two independent modal sources. Each criterion reduces the same cross-PSD to a scalar equivalent stress, evaluated here with the Tovo–Benasciutti damage model. Because the stress amplitudes in this reused dataset are not tied to a specific service load, the loading of each case is scaled to a common reference level so the predicted lives are comparable: the scale factor is set so the EVMS root-mean-square (RMS) equivalent stress equals 60 MPa, safely below the axial fatigue limit $\sigma_{af} = 161$ MPa. The scaling is applied after the criteria are evaluated, so it shifts the absolute lives but leaves the relative spread between criteria unchanged. Figure 1 and Table 2 report the RMS equivalent stress returned by each criterion.

Across the ten criteria the equivalent stress varies by about a factor of 1.6 for the combined bending and torsion state and 1.7 for the normal-dominated state. The three critical-plane criteria coincide for the normal-dominated state and separate once shear is present, where the maximum-shear criterion returns the largest value. The thermoelastic criterion, which combines the normal stress components, is highest for the normal-dominated state and lower when shear dominates. The out-of-phase correction matches the EVMS value here because both datasets are in phase at each frequency. Since fatigue life scales with roughly the inverse fifth to sixth power of stress, this spread in equivalent stress becomes a life spread of about 16 to 18. The comparison uses the same input for every criterion and is produced by changing a single method call. Both datasets and a notebook that reproduces this comparison end to end are distributed with `FLife` [43], so the full example, from the stress cross-PSDs to the figure and table shown here, can be rerun and extended without re-implementing any criterion.

Further progress here is mostly an experimental problem. Without controlled multiaxial random-vibration benchmark datasets, the relative accuracy of phase-sensitive and phase-insensitive criteria cannot be decided [3,29].

The open-source consolidation we provide is meant to remove the coding effort, so that an experimental campaign does not also have to carry out ten reimplementations before a comparison can begin. Smaller open issues remain: the assumption of stationary linear Gaussian response [2], and the need to track modal fatigue response spectra [63] and bimodal PSD parameterisations [64].

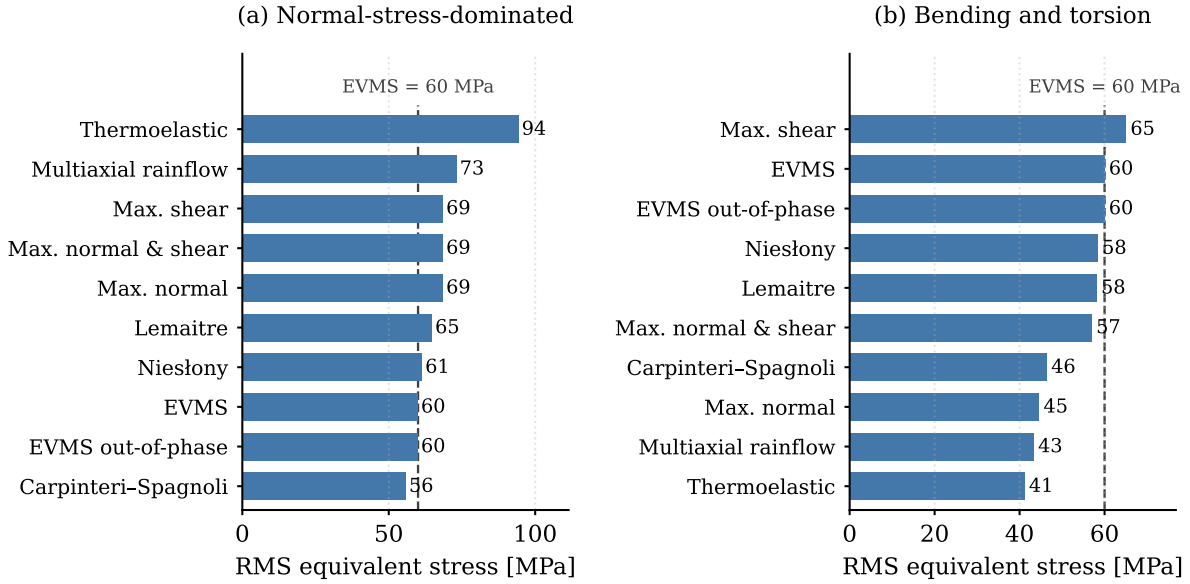

Figure 1. RMS equivalent stress returned by each criterion on the same input, for (**a**) a normal-stress-dominated state and (**b**) a combined bending and torsion state. The loading is scaled so the EVMS value equals 60 MPa (dashed line).

Table 2. RMS equivalent stress and estimated fatigue life per criterion for the two demonstration cases (loading scaled to an EVMS RMS of 60 MPa; Tovo–Benasciutti damage model).

Criterion	(a) Normal-Dominated		(b) Bending + Torsion	
	RMS [MPa]	Life	RMS [MPa]	Life
Max. normal	68.6	1.4 h	44.6	2.1 h
Max. shear	68.6	1.4 h	65.1	13 min
Max. normal & shear	68.6	1.4 h	57.0	29 min
EVMS	60.0	2.9 h	60.0	22 min
Carpinteri–Spagnoli	55.9	4.4 h	46.4	1.6 h
Multiaxial rainflow	73.2	59 min	43.3	2.5 h
Thermoelastic	94.4	14 min	41.2	3.6 h
EVMS out-of-phase	60.0	2.9 h	60.0	22 min
Niesłony	61.4	2.6 h	58.4	26 min
Lemaitre	64.8	1.9 h	58.2	26 min

11. Conclusions

An implementation-oriented review of ten multiaxial spectral criteria for vibration-fatigue life estimation is presented. All ten criteria follow the same two-step pipeline: the stress cross-PSD matrix is reduced to a scalar equivalent PSD, which is then evaluated with a uniaxial spectral damage model. They differ in their treatment of phase information, material-parameter requirements, and computational cost (see Table 1). For proportional loading, simpler criteria such as EVMS provide adequate equivalent-stress estimates; under non-proportional conditions, phase-sensitive formulations can be expected to offer improved accuracy at the cost of added complexity or restricted dimensionality.

All ten criteria are implemented in the open-source package `FLife` [43], which extends the uniaxial spectral-method framework established by Zorman et al. [42]. Within this package, each multiaxial criterion can be paired with any of the more than twenty uniaxial spectral damage models already available [21], enabling reproducible side-by-side comparison of criteria on identical input data within a single consistent workflow. To the authors' knowledge, such a combinatorial evaluation environment has not previously been available in a single open-source package. Using this workflow, the ten criteria were applied to two common datasets: the RMS equivalent stress

spanned a factor of about 1.6 to 1.7 and the estimated life about 16 to 18, with the data and a reproduction notebook shipped with the package. A full experimental accuracy benchmark across materials and loading types remains future work.

Open directions for future work remain. The Bonte and multiaxial-rainflow criteria still require three-dimensional generalisations. The ten criteria range mathematically from scalar trace operations to nonlinear orientation searches, and a unified framework establishing formal equivalences or bounds between them would be valuable. Data-driven method-selection guidelines become practical only once benchmark datasets are available.

Funding

This research was funded by the Slovenian Research and Innovation Agency (ARIS), research core funding No. P2-0263.

Data Availability Statement

The `FLife` package (version 2.2.0) is available at https://pypi.org/project/FLife/ and on GitHub at https://github.com/ladisk/FLife. This release includes the multiaxial module and the notebook that reproduces the numerical comparison of Section 10.1.

Conflicts of Interest

The authors declare no conflict of interest.

Use of AI and AI-Assisted Technologies

We confirm that Claude (Anthropic) was used to assist with language refinement and style polishing of the manuscript text. After using this tool, the authors reviewed and edited the content as needed and take full responsibility for the content of the publication.

References

1. Lalanne, C. *Mechanical Vibration and Shock Analysis*, 3 ed.; Volume 4: Fatigue Damage; ISTE Ltd.: London, UK/John Wiley & Sons: Hoboken, NJ, USA, 2014.
2. Benasciutti, D.; Tovo, R. Frequency-based analysis of random fatigue loads: Models, hypotheses, reality. *Mater. Werkst.* **2018**, *49*, 345–367.
3. Muñiz-Calvente, M.; Álvarez-Vázquez, A.; Pelayo, F.; et al. A comparative review of time- and frequency-domain methods for fatigue damage assessment. *Int. J. Fatigue* **2022**, *163*, 107069.
4. Garud, Y.S. Multiaxial Fatigue: A Survey of the State of the Art. *J. Test. Eval.* **1981**, *9*, 165–178.
5. Bendat, J.S.; Piersol, A.G. *Random Data: Analysis and Measurement Procedures*, 4 ed.; John Wiley & Sons: Hoboken, NJ, USA, 2010.
6. Preumont, A. *Random Vibration and Spectral Analysis*; Kluwer Academic Publishers: Dordrecht, The Netherlands, 1994.
7. Braccesi, C.; Cianetti, F.; Lori, G.; et al. Random multiaxial fatigue: A comparative analysis among selected frequency- and time-domain fatigue evaluation methods. *Int. J. Fatigue* **2015**, *74*, 107–118.
8. Pitoiset, X.; Preumont, A. Spectral methods for multiaxial random fatigue analysis of metallic structures. *Int. J. Fatigue* **2000**, *22*, 541–550.
9. Mršnik, M.; Slavič, J.; Boltežar, M. Multiaxial vibration fatigue—A theoretical and experimental comparison. *Mech. Syst. Signal Process.* **2016**, *76–77*, 409–423.
10. Benasciutti, D.; Sherratt, F.; Cristofori, A. Recent developments in frequency domain multi-axial fatigue analysis. *Int. J. Fatigue* **2016**, *91*, 397–413.
11. Aimé, M.; Banvillet, A.; Khalij, L.; et al. A framework proposal for new multiaxial fatigue damage and extreme response spectra in random vibrations frequency analysis. *Mech. Syst. Signal Process.* **2024**, *213*, 111338.
12. Proner, E.; Mucchi, E.; Tovo, R. A relationship between fatigue damage estimation under multi-axis and single-axis random vibration. *Mech. Syst. Signal Process.* **2024**, *215*, 111402.
13. Proner, E.; Mucchi, E. A multi-axial Fatigue Damage Spectrum for the evaluation of the fatigue damage potential of multi-axis random vibration environments. *Mech. Syst. Signal Process.* **2025**, *226*, 112362.
14. Rychlik, I. A new definition of the rainflow cycle counting method. *Int. J. Fatigue* **1987**, *9*, 119–121.
15. Wirsching, P.H.; Light, M.C. Fatigue Under Wide Band Random Stresses. *J. Struct. Div.* **1980**, *106*, 1593–1607.
16. Dirlik, T. Application of Computers in Fatigue Analysis. PhD Thesis, University of Warwick, Coventry, UK, 1985.
17. Bishop, N.W.M.; Sherratt, F. A theoretical solution for the estimation of “rainflow” ranges from power spectral density data. *Fatigue Fract. Eng. Mater. Struct.* **1990**, *13*, 311–326.

18. Benasciutti, D.; Tovo, R. Spectral methods for lifetime prediction under wide-band stationary random processes. *Int. J. Fatigue* **2005**, *27*, 867–877.
19. Braccesi, C.; Cianetti, F.; Lori, G.; et al. Fatigue behaviour analysis of mechanical components subject to random bimodal stress process: frequency domain approach. *Int. J. Fatigue* **2005**, *27*, 335–345.
20. Zanardi, M.; Cavalca, K.; Pinzi, V.; et al. Dirlik and Tovo–Benasciutti spectral methods in vibration fatigue: a review with a historical perspective. *Mathematics* **2021**, *9*, 1460.
21. Slavič, J.; Mršnik, M.; Česnik, M.; et al. *Vibration Fatigue by Spectral Methods: From Structural Dynamics to Fatigue Damage—Theory and Experiments*; Elsevier: Amsterdam, The Netherlands, 2020.
22. Preumont, A.; Piéfort, V. Predicting Random High-Cycle Fatigue Life With Finite Elements. *J. Vib. Acoust.* **1994**, *116*, 245–248.
23. Benasciutti, D. Some analytical expressions to measure the accuracy of the "equivalent von Mises stress" in vibration multiaxial fatigue. *J. Sound Vib.* **2014**, *333*, 4326–4340.
24. Bonte, M.H.A.; de Boer, A.; Liebregts, R. Determining the von Mises stress power spectral density for frequency domain fatigue analysis including out-of-phase stress components. *J. Sound Vib.* **2007**, *302*, 379–386.
25. Niesłony, A.; Macha, E. *Spectral Method in Multiaxial Random Fatigue*; *Lecture Notes in Applied and Computational Mechanics*; Springer: Berlin/Heidelberg, Germany, 2007; Volume 33.
26. Cristofori, A.; Benasciutti, D.; Tovo, R. A stress invariant based spectral method to estimate fatigue life under multiaxial random loading. *Int. J. Fatigue* **2011**, *33*, 887–899.
27. Niesłony, A. Comparison of some selected multiaxial fatigue failure criteria dedicated for spectral method. *J. Theor. Appl. Mech.* **2010**, *48*, 233–254.
28. Łagoda, T.; Macha, E.; Bedkowski, W. A critical plane approach based on energy concepts: application to biaxial random tension-compression high-cycle fatigue regime. *Int. J. Fatigue* **1999**, *21*, 431–443.
29. Carpinteri, A.; Spagnoli, A.; Vantadori, S. A review of multiaxial fatigue criteria for random variable amplitude loads. *Fatigue Fract. Eng. Mater. Struct.* **2017**, *40*, 1007–1036.
30. Angeli, E.; Cornelis, B.; Troncossi, M. Sine-on-Random vibration profiles for accelerated life tests: Ensuring Fatigue Damage Spectrum equivalence. *Mech. Syst. Signal Process.* **2018**, *103*, 340–351.
31. Wolfsteiner, P.; Breuer, W. Fatigue assessment of vibrating rail vehicle bogie components under non-Gaussian random excitations using power spectral densities. *J. Sound Vib.* **2013**, *332*, 5867–5882.
32. Wolfsteiner, P.; Trapp, A. Modeling of statistical and spectral properties of non-Gaussian random vibration fatigue loads using Higher Order Spectra. *Int. J. Fatigue* **2025**, *198*, 109004.
33. Trapp, A.; Wolfsteiner, P. Fast assessment of non-Gaussian inputs in structural dynamics exploiting modal solutions. *Mech. Syst. Signal Process.* **2025**, *228*, 112396.
34. Palmieri, M.; Slavič, J.; Cianetti, F. Fast evaluation of central moments for non-Gaussian random loads in vibration fatigue. *Mech. Syst. Signal Process.* **2025**, *228*, 112434.
35. Lei, W.; Jiang, Y.; Tian, Y.; et al. Kurtosis transfer in MDOF systems under amplitude-modulated non-stationary non-Gaussian excitations: A frequency-domain decomposition approach. *Mech. Syst. Signal Process.* **2025**, *236*, 113059.
36. Cui, S.; Chen, S.; Li, J.; et al. Integrating mean stress correction into a non-Gaussian spectral method for fatigue damage estimation. *Int. J. Fatigue* **2026**, *209*, 109604.
37. Sgamma, M.; Palmieri, M.; Barsanti, M.; et al. Study of the response of a single-dof dynamic system under stationary non-Gaussian random loads aimed at fatigue life assessment. *Heliyon* **2024**, *10*, e30832.
38. Gao, D.; Huang, Y.; Liao, W. A critical distance parameter for random vibration fatigue life estimation of notched metallic structures in the frequency domain. *Int. J. Mech. Syst. Dyn.* **2025**, *5*, 101–112.
39. Steengaard, J.R.; Avendaño Valencia, L.D.; Lützen, M.; et al. Comparison of uniaxial spectral methods for weld fatigue. *Int. J. Fatigue* **2026**, *209*, 109656.
40. Lu, H.; Lian, Y.; Wang, J.; et al. Fatigue assessment of directionally solidified superalloy thin plates under bimodal random processes. *Thin-Walled Struct.* **2024**, *205*, 112411.
41. Cui, D.; Xie, R.; Li, M.; et al. A novel framework for fatigue hotspot localization and damage assessment of multi-defect marine structures under random vibration. *Ocean. Eng.* **2025**, *316*, 119982.
42. Zorman, A.; Slavič, J.; Boltežar, M. Vibration fatigue by spectral methods—A review with open-source support. *Mech. Syst. Signal Process.* **2023**, *190*, 110149.
43. Zorman, A.; Šonc, J.; Mršnik, M.; et al. FLife: Vibration Fatigue by Spectral Methods (Version 2.2.0). 2026. Available online: https://pypi.org/project/FLife/2.2.0/ (accessed on 26 May 2026).
44. Niesłony, A.; Böhm, M.; Owsiński, R.; et al. Integrating von Mises and hydrostatic stresses in frequency domain multiaxial fatigue criteria for vibration fatigue analysis. *Mech. Syst. Signal Process.* **2025**, *224*, 112229.
45. Ge, J.; Sun, Y.; Zhou, S. Fatigue life estimation under multiaxial random loading by means of the equivalent Lemaitre stress and multiaxial S–N curve methods. *Int. J. Fatigue* **2015**, *79*, 65–74.
46. Šonc, J.; Zaletelj, K.; Slavič, J. Application of thermoelasticity in the frequency-domain multiaxial vibration-fatigue criterion. *Mech. Syst. Signal Process.* **2025**, *224*, 112002.
47. Pei, X.; Cao, Y.; Gu, T.; et al. Generalizing multiaxial vibration fatigue criteria in the frequency domain: A data-driven

approach. *Int. J. Fatigue* **2024**, *186*, 108390.
48. Zhang, Z.; Pan, Y.; Zhou, X.; et al. Multiaxial random vibration life prediction framework via damage correction factor. *Int. J. Mech. Sci.* **2026**, *309*, 111047.
49. Findley, W.N. A Theory for the Effect of Mean Stress on Fatigue of Metals Under Combined Torsion and Axial Load or Bending. *J. Eng. Ind.* **1959**, *81*, 301–305.
50. Brown, M.W.; Miller, K.J. A Theory for Fatigue Failure under Multiaxial Stress-Strain Conditions. *Proc. Inst. Mech. Eng.* **1973**, *187*, 745–755.
51. Pitoiset, X.; Rychlik, I.; Preumont, A. Spectral methods to estimate local multiaxial fatigue failure for structures undergoing random vibrations. *Fatigue Fract. Eng. Mater. Struct.* **2001**, *24*, 715–727.
52. Matake, K. An explanation on fatigue limit under combined stress. *Bull. Jpn. Soc. Mech. Eng.* **1977**, *20*, 257–263.
53. Carpinteri, A.; Spagnoli, A.; Vantadori, S. Reformulation in the frequency domain of a critical plane-based multiaxial fatigue criterion. *Int. J. Fatigue* **2014**, *67*, 55–61.
54. Carpinteri, A.; Spagnoli, A. Multiaxial high-cycle fatigue criterion for hard metals. *Int. J. Fatigue* **2001**, *23*, 135–145.
55. Matsuishi, M.; Endo, T. Fatigue of Metals Subjected to Varying Stress. In Proceedings of the Japan Society of Mechanical Engineers; Japan Society of Mechanical Engineers: Fukuoka, Japan, 1968; pp. 37–40.
56. Endo, T.; Mitsunaga, K.; Takahashi, K.; et al. Damage Evaluation of Metals for Random or Varying Loading: Three Aspects of Rain Flow Method. In Proceedings of the 1974 Symposium on Mechanical Behavior of Materials, Kyoto, Japan, 21–24 August 1974; Volume 1, pp. 371–380.
57. Beste, A.; Dressler, K.; Kötzle, H.; et al. Multiaxial Rainflow—A Consequent Continuation of Professor Tatsuo Endo's Work. In *The Rainflow Method in Fatigue: The Tatsuo Endo Memorial Volume*; Butterworth-Heinemann: Oxford, UK, 1992; pp. 31–40.
58. Dressler, K.; Köttgen, V.B.; Kötzle, H. Tools for fatigue evaluation of non-proportional loading. *Fatigue Des.* **1995**, *1*, 261–277.
59. Pitarresi, G.; Patterson, E.A. A review of the general theory of thermoelastic stress analysis. *J. Strain Anal. Eng. Des.* **2003**, *38*, 405–417.
60. Dulieu-Barton, J.M. Introduction to thermoelastic stress analysis. *Strain* **1999**, *35*, 35–39.
61. Lemaitre, J.; Desmorat, R. *Engineering Damage Mechanics: Ductile, Creep, Fatigue and Brittle Failures*; Springer: Berlin/Heidelberg, Germany, 2005.
62. Susmel, L.; Lazzarin, P. A bi-parametric Wöhler curve for high cycle multiaxial fatigue assessment. *Fatigue Fract. Eng. Mater. Struct.* **2002**, *25*, 63–78.
63. Sui, G.; Jin, X.; Cui, H.; et al. Improvement and test verification of the fatigue response spectrum method. *Mech. Syst. Signal Process.* **2024**, *217*, 111519.
64. Curti, G.; Palmieri, M.; Cianetti, F. Towards systematic random process representation: Bimodal PSDs characterized by bandwidth indices. *Int. J. Fatigue* **2026**, *204*, 109359.